

# **Adsorption properties of plant based bio-surfactants: insights from neutron scattering techniques.**

J Penfold<sup>1,2,\*</sup>, R K Thomas<sup>1</sup>

## **ABSTRACT**

There is an increasing interest in biosustainable surfactants and surface active proteins for a range of applications, in home and personal care products, cosmetics, pharmaceuticals, and food and drink formulations. This review focuses on two plant derived biosurfactants, the surface active glycoside, saponin, and the surface active globular protein, hydrophobin. A particular emphasis in the review is on the role of neutron reflectivity in probing the adsorption, structure of the adsorbed layer, and their mixing at the interface with a range of more conventional surfactants and proteins.

1. Physical and Theoretical Chemistry Dept, University of Oxford, South Parks Road, Oxford, UK
2. ISIS Facility, STFC, Rutherford Appleton Laboratory, Chilton, Didcot, OXON, UK

- Corresponding Author: Jeff Penfold, email: [jeff.penfold@stfc.ac.uk](mailto:jeff.penfold@stfc.ac.uk)

## **1. GENERAL INTRODUCTION.**

Although the original production of surfactants derived from a range of plant and animal based sources, it is synthetic surfactants, derived from mainly petrochemical or oleochemical sources, that have dominated surfactant production for at least the last century. In recent years there has been an increasing interest in biosustainable and biocompatible surfactants, natural surfactants that can be derived from and synthesised from renewable feedstocks and sustainable sources (1-3). Holmberg (1) discussed the narrow definition of natural surfactants, as derived from plant or animal origin by some extraction route, and which does not involve further synthesis. However the wider definition involves the synthesis of surfactants from raw materials derived from plant or animal components, and which may involve organic synthesis or some bacterial route. The subject of this review are biosurfactants that come from that narrower definition of natural surfactants and have been extracted from plant and fungal based sources.

The term biosurfactant covers this wide range of naturally occurring surfactants or surfactants synthesised from natural components, that are water soluble surface active species. The two main characteristics which all surfactants possess are their strong surface activity, adsorption to different interfaces and surfaces, and their ability to self-assemble into aggregates, micelles or a variety of liquid crystalline phases at higher solution concentrations. In synthetic surfactants the main structural characteristics are a hydrophilic group which may be charged, anionic or cationic, or uncharged, nonionic; and a hydrophobic group which is usually an alkyl chain. In biosurfactants the headgroup can consist of amino acids or saccharide groups, and the hydrophobic portion could be an alkyl chain, a group of hydrophobic amino acids or a triterpenoid, steroidal or steroid-alkaloid group. A distinct separation between the hydrophilic and hydrophobic regions is often less clear cut in some biosurfactants. There are a number of ways and criteria by which to classify biosurfactants, but Roz and Rosenberg (4) provided a useful classification of biosurfactants based simply on molecular weight. The low molecular weight biosurfactants are typically glycolipids or lipopeptides and are usually bacterial based (3). The higher molecular weight biosurfactants are often biopolymers, such as polysaccharides, proteins, liposaccharides, or lipoproteins, and are mainly exocellular. Biosurfactants are a complex mixture of structural variations, and this polydispersity in structure will have implications; as

will be discussed later in the review. The particular focus of this review are two different classes of biosurfactant with intermediate MW's, in the range  $\geq 500$  and  $\sim 10\text{k Da}$ ; and are the saponins (5) and hydrophobins (6). The saponins are glycosides which are widely found in many plant species, and have structures containing a steroidal or triterpenoid glycone and one or more sugar groups (5). In contrast, the hydrophobins are proteins produced by filamentous fungi (6), and are highly surface active due to their asymmetrical distribution of hydrophilic and hydrophobic amino acids on a compact globular protein surface.

The biological functions of biosurfactants are not always entirely clear (7). However their ability to reduce interfacial tensions, wet interfaces and act as efficient emulsifiers are all criteria required for biofilm growth, and the increased bioavailability of carbon required for bacterial growth in bacterial based biosurfactants. Specific antibacterial and antimicrobial properties are involved in bacteria pathogenesis, quorum sensing and in biofilm growth. As such many biosurfactants have been exploited in specialist and niche applications, in bioremediation of spoils of hydrocarbons, heavy metals and pesticides, in a wide range of food formulation requiring good foam or emulsion stability, and in cosmetics (8-11). However the main attraction of biosurfactants in terms of wider application and in the replacement of synthetic surfactants lies in their biocompatibility and biosustainability, and to a lesser extent in specific properties not accessible to synthetic surfactants. However, apart from the application in some specialised high added value applications, the wider application of biosurfactants depends upon the development of cheap large scale production, separation and purification (9). Increasingly there is a realisation that the wider application of biosurfactants will at least initially involve mixtures with conventional synthetic surfactants. To optimise such blending it is essential that the physico-chemical properties of biosurfactants are better characterised. An important aspect of that is the surface adsorption properties of biosurfactants and biosurfactant / surfactant mixtures. For us the technique of choice for studying surfactant and mixed surfactant adsorption is neutron reflectivity (12), and this is the other main focus of this review. Neutron reflectivity provides direct information about adsorbed amounts, the surface composition of surfactant mixtures, and the structure of the adsorbed layer; and has been extensively applied to surfactant (12) and mixed surfactant (12, 13) adsorption. As will be discussed in more detail in the next section a key feature in the application of neutron reflectivity to study surfactant

adsorption has been the ability to manipulate the neutron refractive index by deuterium labelling the surfactant and / or the solvent. The application of neutron reflectivity to some biosurfactants was recently reviewed by Penfold et al (14). Neutron reflectivity has been successfully applied in the study of two glycolipid biosurfactants, rhamnolipids (15-18), and sophorolipids (19), and the lipopeptide surfactin (20, 21). However, initially through mainly the study of protein adsorption (22-25) using neutron reflectivity, there is an increasing realisation that for the proteins, lipopeptides, lipoproteins, and glycosides deuterium labelling is not a limiting requirement.

The focus of this review is on the application of neutron reflectivity to study two biosurfactants at the air-solution interface, the glycoside saponin, and the globular protein hydrophobin, and the mixing of hydrophobin with a range of conventional surfactants. In the examples presented both the adsorbed amounts and the structure of the adsorbed layer will be determined and interpreted.

## 2. NEUTRON REFLECTIVITY

The wave nature of thermal neutrons is well established, and as a consequence neutrons exhibit all the familiar optical phenomena of reflection, refraction and interference in thin films (26). Hence the same formalisms established for the optical properties of thin films (26, 27) can be applied to neutrons. Thermal / cold neutrons typically have wavelengths  $\sim 1$  to  $20 \text{ \AA}$ , and so at grazing incidence length scales  $\sim 10$  to  $2000 \text{ \AA}$  are accessible (28). Neutron reflectivity from a planar surface can be considered as a depth profiling technique which provides information about the structure and composition of surfaces / interfaces in the direction perpendicular to the surface. In the kinematic approximation, and by analogy with scattering theory, the variation in the reflectivity with wave vector transfer,  $Q$ , (where  $Q=4\pi \sin\theta / \lambda$ ,  $\theta$  is the grazing angle of incidence and  $\lambda$  is the neutron wavelength) normal to the surface is given by,

$$R(Q) = \frac{16\pi^2}{Q^2} \left| \int \rho(z) e^{-iQz} dz \right|^2 \quad (1)$$

and  $\rho(z)$  is the neutron scattering length density distribution which is related to the density distribution by the neutron scattering lengths of the different components at the interface. This approach has been extensively applied to the study of surfactant and surfactant

mixtures adsorbed at interfaces (12, 13). The key to its success has been the manipulation of the neutron refractive index, 'contrast', via  $\rho(z)$  by deuterium labelling of the adsorbate and / or solvent (D and H have very different neutron scattering lengths). For example, for a deuterium labelled surfactant in null reflecting water, nrw, (92 mol% D<sub>2</sub>O / 8 mol% H<sub>2</sub>O, which has a  $\rho$  of 0.0 identical to air) a relatively easily detectable reflectivity signal arises only from the adsorbed layer. Treating that layer as a single uniform layer of thickness  $d$  and scattering length density  $\rho$  provides a direct determination of the adsorbed amount via the adsorbed amount  $A$ , where  $A = \sum b/d\rho$ , and  $\sum b$  is the sum of scattering lengths of the adsorbed molecule. It is straightforward to extend this to mixtures, where  $A_i = \sum b_i/d_i\rho_i$  for the  $i$ th component; and by selective deuteration of each component the composition of a multicomponent mixture can be determined (12). More elaborate labelling schemes can be used to determine the structure of the adsorbed layer in more detail, to determine the extent of solvent penetration, surfactant configuration and the relative positions of the components in mixtures (12).

However, in the context of this review and the application of neutron reflectivity to protein, lipoprotein and glycoside adsorption, recent developments in instrumentation and neutron sources mean that such surface active species can be investigated without the need for deuterium labelling. Manipulating the solvent contrast can also often give further insights into the structure of the adsorbed layer in such systems. It will be shown how this has been exploited to study saponin and hydrophobin adsorption. In the case of hydrophobin studies of hydrophobin / surfactant adsorption have relied upon deuterium labelling of the conventional surfactant to obtain surface compositions and more detailed structural information.

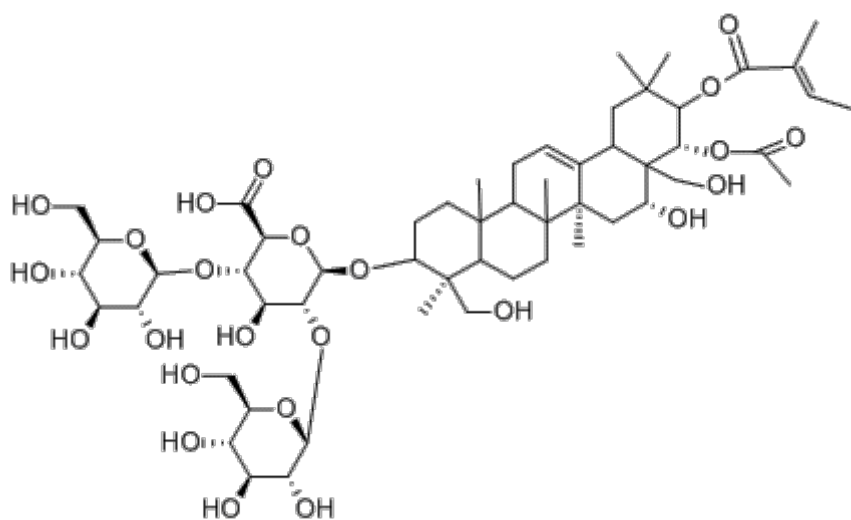
### **3. SAPONINS**

#### **3.1 Introduction**

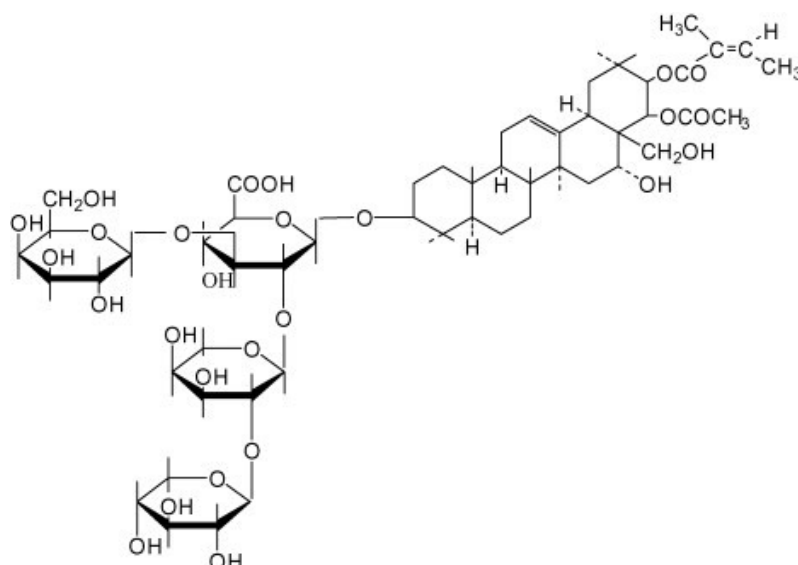
Saponins are non-volatile surface active components that are found extensively in nature in a wide variety of plant species (30-33). They are glycosides with molecular structures that contain a steroidal or triterpenoid aglycone hydrophobic region and a hydrophilic portion which contains one or more sugar groups; and this hydrophilic / hydrophobic separation is the origin of their surface activity. A wide range of different structures exist, depending

upon the different plant species of origin. This gives rise to a rich range of physicochemical properties and different biological activities. Even within a specific saponin type there will be a range of structural variations, and properties will vary according to the extent of that polydispersity and the extraction / purification process. The current interest arises from their original use in soaps, the name saponin is from the latin for soap, *sapo*, and in a variety of applications in natural medicines; and has given rise to a number of recent review articles (30-34).

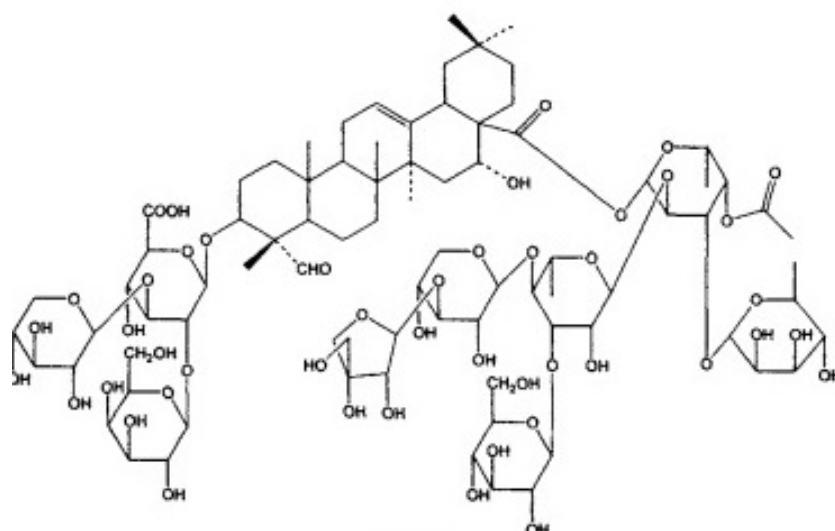
The structure of some of the more commonly investigated and exploited saponins, Escin, Tea, and Quillaja, are shown in figure 1. They are also the focus of this section and of our recent neutron reflectivity studies.



(a)



(b)



(c)

**Figure 1.** Molecular structure of saponins (a) Escin, (b) Tea and (c) Quillaja

The saponin glycosides are classified in terms of the type of hydrophobic portion which is either a triterpenoid, steroidal or steroid-alkaloid group. Attached to this hydrophobic scaffold via glycoside bonds are a range of different saccharide groups. These may be mono-, di-, or tri-desmosidic, comprising one, two, or three sugar groups. In figure 1 the Escin and Tea saponins are monodesmosidic, whereas the Quillaja saponin is bidesmosidic. The sugar groups can be a range of different monosaccharides, and include commonly, glucose, galactose, rhamnose, arabinose, xylose and fructose (30). The structural complexity and variations available give rise to the broad physical, chemical and biological properties and applications reported (30-34).

The surface activity of saponins is the basis of their use as emulsifiers and foam stabilisers in foods and beverages (30, 33, 35, 36). Example of this are that saponins are currently used to stabilise foams in some beers and soft drinks (30, 35), and as stabilising agents for different food additives (36). In the home and personal care sector they have been used as stabilisers in cosmetic emulsions and creams, shampoos and conditioners, and in skin anti-ageing products (30, 33, 37). The biological activity of saponins is diverse and saponins possess anti-inflammatory, anti-fungal, anti-bacterial properties, and haemolytic activity. Such factors have made them popular ingredients in natural medicines (32, 38, 39), and more

recently for anti-cancer and cholesterol lowering functions (32, 40). They are also an attractive starting point for the synthesis of steroid based drugs by the pharmaceutical industry (32).

The abundance of saponins in many plants and their presence in many processing by-products presents a great opportunity for wider commercial exploitation. As such they are being more extensively exploited in the food, cosmetics and pharmaceutical sectors. Greater exploitation requires a more detailed understanding of their adsorption and self-assembly properties, how they vary with the different saponin structures and how they interact with other components. We review here some aspects of that characterisation and especially how those recent studies relate to the more recent applications of neutron reflectivity to the study of saponin adsorption.

### **3.2 Surface Rheology and surface tension**

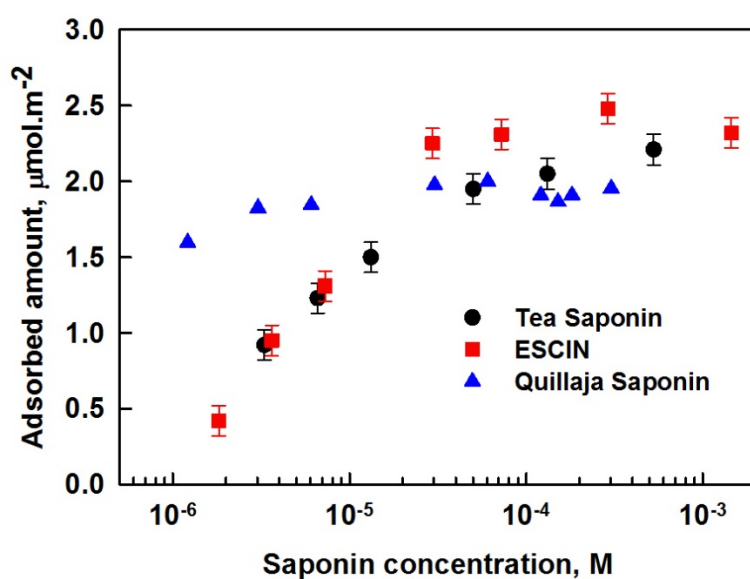
The saponins have demonstrated a particular ability to stabilise foams and emulsions, and many of their current applications stem from that. Apart from their intrinsic surface activity the saponins exhibit some unusual surface properties, in that the surface layers have high surface dilational moduli and shear viscoelasticity. The surface rheology of saponin solutions has hence been a major focus of recent studies (41,42,44,45). Pagureva et al (41) and Golemanov et al (45) studied the surface rheological properties, both shear and dilational, of a range of triterpenoid and steroidal saponins, which included Tea, Escin, Berry, Ginsenoside and Quillaja saponins. Although surface tension measurements are challenging with such extreme surface rheology, Pagureva et al (41) extracted from dynamic and static surface tension measurements adsorbed amounts for the triterpenoid saponins, Tea, Escin, Berry, with area/ molecules in the range 50 to 70 Å<sup>2</sup>. They assumed, from packing considerations, but without any independent structural information at that stage, that the molecules were oriented perpendicular to the surface. The Tea, Escin and Berry saponins all exhibit viscoelastic surface behaviour (41, 45), and have high dilational and shear viscosities. In these mainly monodesmosidic triterpenoid saponins extreme viscoelastic properties are attributed to a dense adsorbed layer and a strong attractive force between neighbouring saponin molecules. It was assumed that the strong interaction between the saponin molecules in the adsorbed layer arises from hydrogen bonds between neighbouring saccharide groups. In contrast to the triterpenoid saponins the steroid based saponins are



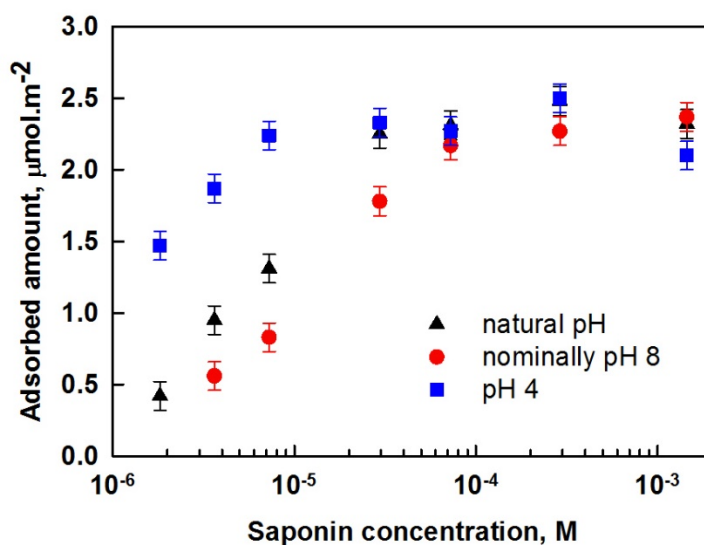
unable to form strong intermolecular bonds in the adsorbed layer and have zero shear elasticity and viscosity and low dilational elasticity and viscosity, comparable to that observed in some protein layers. Furthermore the less compact bidesmosidic and tridesmosidic saponins exhibited less extreme surface rheological properties, as the larger bulkier sugar residues are likely to partially inhibit the formation of compact adsorbed layers. An example of this is the Quillaja saponin which is bidesmosidic and which has a more extensive headgroup structure (see figure 1c). Surface tension measurements indicate an area / molecule  $\sim 100 \text{ \AA}^2$  for the Quillaja saponin (42). A range of area / molecule from Quillaja Bark saponins, in the range 40 to  $120 \text{ \AA}^2$ , was reported by Wociechowski (43), depending upon the saponin source; and we will return to this point when discussing the structure of the adsorbed saponin layers. Stanimirova et al (42) and Golemanov et al (44) have reported in depth on the surface rheology of the Quillaja saponin. The Quillaja saponin exhibited a high surface dilational elasticity, a low shear elasticity and a negligible dilational viscosity. Clearly the detailed nature of the adsorbed layer has an important impact upon the surface rheology. With that in mind Tsibranska et al (46) have used molecular dynamics to study the nature of the adsorbed saponin layer at the air-water interface, and we will return to this when discussing recent related neutron reflectivity data (47).

### **3.3 Neutron reflectivity adsorption studies**

Neutron reflectivity measurements were made at the air-water interface for the Escin, Tea, and Quillaja saponins by Penfold et al (47). The compositions of the saponins are such that there is sufficient reflectivity in nrw ( $\Sigma b$  for the saponins varies from 1.8 to  $3 \times 10^{-3} \text{ \AA}$ ) without the need for deuterium labelling of the saponin. The reflectivity data are consistent with an adsorbed layer of thickness  $\sim 26 \text{ \AA}$ .



(a)



(b)

**Figure 2.** (a) Adsorbed amount versus concentration for Tea, Escin and Quillaja saponins at the air-water interface (see legend for details), (b) Adsorbed amount versus concentration for Escin at different solution pH (see legend for details). Reproduced from reference 47.

At natural pH the adsorption isotherms for Escin, Tea and Quillaja saponins are shown in figure 2a, and the mean area/molecule at saturation are  $69$ ,  $79$  and  $87 \pm 5 \text{ \AA}^2$  respectively. The mean area / molecule increases with the molecular weight of the saponin. The surface saturation occurs at a similar concentration for the Escin and Tea saponins, consistent with

them containing similar hydrophobic fragments. The surface saturation for the Quillaja saponin occurs at a much lower concentration, and reflects the bidesmosidic structure of the Quillaja saponin with the additional hydrophobic fragment. The adsorption isotherms for Escin were also measured at different pH, see figure 2b, and the saturated area / molecule values were  $75, 69$  and  $61 \pm 4 \text{ \AA}^2$  at pH 8, natural pH, and pH 4. Although there is a systematic variation, within the error in the measurement the adsorption above the critical micelle concentration, CMC, is largely independent of pH with a mean area/molecule  $\sim 69 \pm 4 \text{ \AA}^2$ . However a more significant change with pH is observed below the CMC, as the pH decreases from 8 to 4 the onset of saturation occurs at a lower concentration. This implies that the saponin Escin does not behave entirely as a nonionic-like surfactant, due to the presence of the carboxylic group on the sugar residue. The results show that although the saturation adsorption is determined largely by the molecular dimensions, the charge has a major effect on the adsorption below saturation. Although the adsorbed amounts derived from surface tension (45, 47) are in broad agreement with the neutron reflectivity data, even though the saponin is only weakly ionic it will have implications for the interpretation of the surface tension data.

A more detailed evaluation of the neutron reflectivity data was made in order to elucidate in more detail the structure of the adsorbed layer at saturation. A more accurate determination of the thickness of the layer from the data in nrw alone, by evaluating the variation of 'goodness of fit' with thickness, revealed a systematic difference between the Escin and Tea saponins, with thicknesses of  $28 \pm 2$  and  $30 \pm 2 \text{ \AA}$ . Further measurements in D<sub>2</sub>O and in a D<sub>2</sub>O / H<sub>2</sub>O mixture with a scattering length density between D<sub>2</sub>O and that estimated for the hydrated headgroup region, provided a two layer model consistent with all the data measured at the different solvent contrasts. The resulting structures are visualised in figure 3. For Escin the two layers are composed of the aglycone hydrophobic portion adjacent to the air phase with a thickness  $\sim 8 \text{ \AA}$  and a volume fraction  $\sim 0.3$ ; and the oligosaccharide chain adjacent to the water phase with a thickness  $\sim 14 \text{ \AA}$  and a volume fraction  $\sim 0.8$ . The high volume fraction of the oligosaccharide layer shows that it is composed mostly of the hydrated sugar groups. The dimensions imply that the aglycone region is tilted and partially hydrated (see figure 3a). The recent molecular dynamics simulations (46) provided structures that are consistent with these neutron reflectivity data.

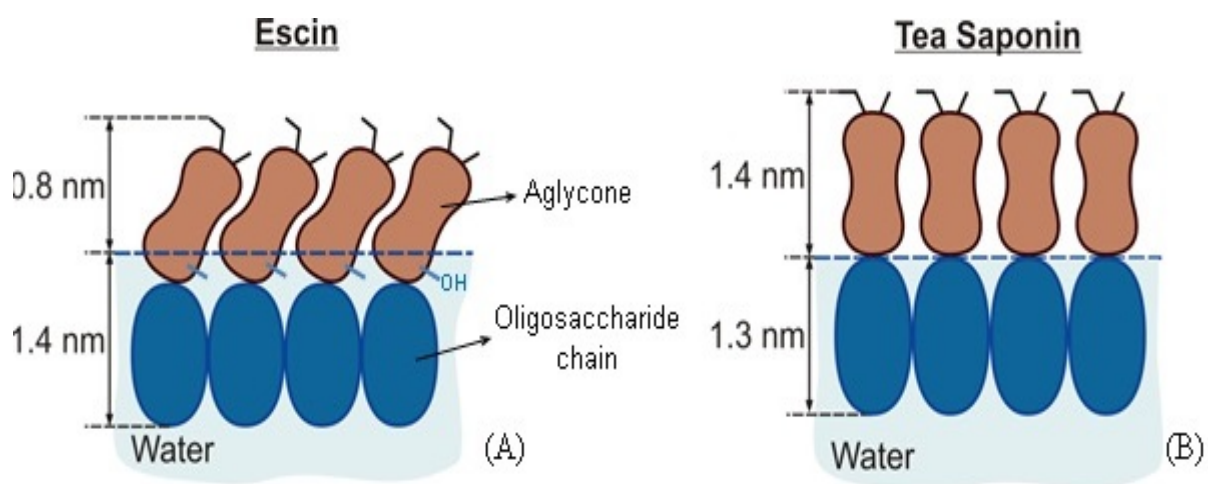


**Figure 3.** Schematic representation of the structure of the Escin (a) and Tea (b) saponins, consistent with the scattering length density profiles determined from the neutron reflectivity data (47). Reproduced from reference 47.

In contrast the Tea saponin data can be described by a similar two layer model, but with corresponding thicknesses of 14 and 13 Å respectively for the aglycone and oligosaccharide regions. The aglycone region has a volume fraction  $\sim 0.4$  and the headgroup region has a volume fraction  $\sim 0.65$ . The dimensions suggest that the Tea saponin portions are more fully extended than in the Escin saponin. In both cases the volume fraction of the oligosaccharide chains in the inner hydrated region is high. This supports the hypothesis that the high surface elasticity of those layers arises from the strong intermolecular hydrogen bonding between the neighbouring sugar groups which is made possible by the dense packing. The difference in the structure between the Escin and Tea saponins reflects the difference in the molecular structures, and is particularly associated with the extra sugar group in the Tea saponin and the additional hydroxyl group in the triterpenoid region of the Escin. For both saponins the outer hydrophobic layer is not so densely packed, and illustrates that the saturation adsorption is determined predominantly by the close packing of the hydrated sugar groups.

Wojciechowski and coworkers (48, 50) have also used neutron reflectivity to study the adsorption of a Quillaja saponin at the air-water and silica water interfaces (48) and their interaction with phospholipids and cholesterol in monolayers (49). Wojciechowski et al (48) reported a relatively thin Quillaja layer at the air-water interface,  $\sim 19$  Å, using neutron reflectivity, which also led to a smaller adsorbed amount compared to surface tension. This

was attributed by them to the extensive hydration of the sugar groups. Furthermore they reported a weaker adsorption at the hydrophilic silica surface. Their results at the air-water interface are not consistent with those reported by Penfold et al (47), but it should be noted that the saponins were from different sources. Penfold et al (47) also only made adsorption isotherm measurements for the Quillaja saponin, and did not make the more detailed structural measurements due to the greater uncertainty in the level of purity of the Quillaja saponin. This uncertainty was highlighted by Wojciechowski (43) when remarking on the variability arising from the different Quillaja sources. Although the correspondence between the surface tension and neutron reflectivity derived adsorbed amount was reasonable in the study by Penfold et al (47), the greatest discrepancy between the two was for the Quillaja saponin. Wojciechowski et al (49, 50) used neutron reflectivity to probe the membranolytic activity of a range of different triterpenoid saponins,  $\alpha$ -hedern, hederaoside C and ammonium glycyrrhizate; studying their adsorption at the air-water interface and phospholipid, DPPC, and DPPC / Cholesterol monolayers. The results indicated a correlation between surface activity and membrane interaction. They also studied the bulk saponin / lipid complex formation. The self-assembly and bulk interactions of saponins are an important feature along with the adsorption and some preliminary studies have been made (51, 52). In particular Mitra and Dugan (51) have studied the temperature, salt and pH effects on the micellar properties of the Quillaja saponin using dynamic light scattering. Both the CMC and hydrodynamic radius varied with temperature and pH, and with the source of saponin. This later variation probably reflects the importance of the exact structure, polydispersity of the system and the inherent purity of the sample. Although the self-assembled nature of the saponins and its variation with solution conditions was well established a more detailed structural characterisation using SAXS or SANS is required.

### **3.3 Adsorption of saponin / surfactant and saponin / protein mixtures**

As highlighted in the Introduction the wider application of saponins will almost certainly rely on their mixing properties with other surface active agents; either conventional surfactants or proteins. Neutron reflectivity is an ideal probe for studying surfactant mixing at interfaces (12, 13), and recent studies on biosurfactant / surfactant mixtures (18) have highlighted the sensitivity that is available using that approach. In the meantime some pioneering studies, using surface tension, light scattering, and other techniques, have been

made on saponin / surfactant (53) and saponin / protein mixtures (54-57), and have demonstrated some synergistic interactions. Jian et al (53), using surface tension and foaming efficiency, established the extent of the synergistic interaction between the Tea saponin and some conventional surfactants, anionic, cationic and nonionic. The variation in CMC was analysed using the Regular Solution Approximation to obtain highly negative interaction parameters in the surface adsorption and micellisation of saponin / cetyl trimethyl ammonium bromide, CTAB and saponin / sodium dodecyl sulfate, SDS mixtures. However, the studies in saponin mixing have predominantly been made with a range of food related proteins and surfactants (54-57), and almost exclusively concern the quillaja saponin. From light scattering, surface tension and conductance measurements Kezwon et al (54) reported synergistic interactions for the saponin with lysozyme,  $\beta$ -lactoglobulin, and  $\beta$ -casein. Piotrowski et al (55) observed condition dependent synergies with  $\beta$ -lactoglobulin, attributed to the adsorption of saponin / protein complexes. Reichart et al (56) investigated the emulsifying properties, oil-in-water emulsions, for the Quillaja saponin with a range of food grade surfactants, which included lecithin and sodium caseinate, and reported synergies due to the formation of mixed interfaces. Wojciechowski et al (57) reported synergies in the adsorption, derived from surface tension, and foamability in Quillaja / Lysozyme mixtures. These studies suggest a rich area for further more detailed investigations, and in which neutron reflectivity would be the technique of choice. We will discuss more generally the nature of protein / surfactant mixing at interfaces in the context of hydrophobin / surfactant mixtures in the next section.

## **4. HYDROPHOBIN**

### **4.1 Introduction.**

Hydrophobins are small highly surface active globular proteins which have attracted much current interest for their potential applications and biological functions (58). Their potential applications have focussed so far on their use as protective coatings and agents and in adhesion. Furthermore their adsorption properties make them attractive for stabilising foams and emulsions in aerated foods, such as ice cream. Hydrophobin is a compact and highly robust protein with a molecular weight in the range 7 to 10 kDa. Its primary crystal structure is known (59, 60), and the protein is globular with a central  $\beta$ -barrel and a small  $\alpha$ -helix segment. It has eight cysteine residues which make four intra-molecular disulphide

bridges. This makes the protein compact, robust and resistant to denaturation. Its surface activity arises mainly from a hydrophobic patch which occupies  $\sim 20\%$  of the surface area, and is comprised of side chain residues of leucine, valine and alanine. The molecular structure of hydrophobin is shown in figure 4.

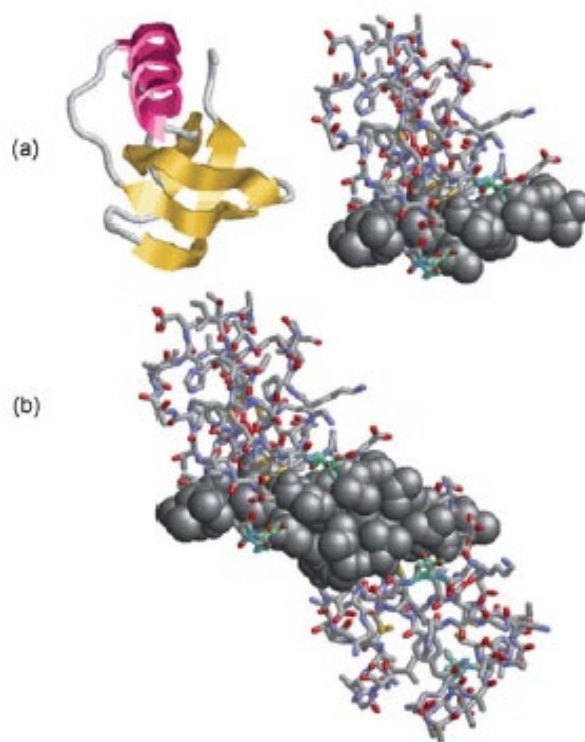


**Figure 4.** Structure of hydrophobin, HFB2, (a) Monomer showing  $\beta$ -sheet and  $\alpha$ -helix region and the hydrophobic patch, (b) dimeric form found in the monoclinic crystalline structure (58-60). Reproduced from reference 14.

This asymmetry in the protein surface and the compact robust nature of the protein have given rise to surface properties that have been compared with Janus particles (61, 62). The hydrophobins are derived from a variety of fungal sources and exist as two main classes, HFB1 and HFB2. HFB1 is more hydrophobic, whereas HFB2 is more water soluble and is the focus in this review; and will be referred to as either HFB2 or simply hydrophobin. Hydrophobins are secreted at and within fungal structures and are associated with different fungal functionalities. Their strong surface activity is central to their function where lowering interfacial tension aids the growth of aerial hyphae, facilitates the attachment of fungal spores to solid surfaces and enables the coating of spores (58). Hence it is the

unusual and remarkable surface properties of hydrophobin, forming highly elastic films, that has attracted much attention and is the focus in this review.

## 4.2 Hydrophobin adsorption

A number of studies have focussed on the surface properties at the air-water interface and on solid surfaces using a variety of surface techniques (61, 63-67); and include surface tension, bubble stability, x-ray reflectivity and grazing incidence diffraction, GIXD, and AFM. Cox et al (61, 63) highlighted the difficulties of obtaining reliable reproducible surface tension data due to the high elasticity of the surface films. This inspired the analogy with Janus particles and was manifest in enhanced bubble stability. The solution self-assembly of the hydrophobins was described in terms of dimers and tetramers, from the SAXS study by Kisko et al (68), and later reinforced by Zhang et al (69) using SANS. With this in mind the adsorption, especially at solid surfaces, was often described as self-assembled films (64-68). The x-ray reflectivity and GIXD data suggest that spread layers of HFB2 at the air / water interface form an hexagonal lattice with a thickness  $\sim 24$  to  $28 \text{ \AA}$ , depending upon the surface pressure, and an area / dimer  $\sim 450 \text{ \AA}^2$ . As part of a wider study of HFB2 / surfactant mixing at interfaces Zhang et al (70, 71) used neutron reflectivity to characterise the adsorption of HFB2 at the air / water and hydrophilic and hydrophobic solid surfaces, without the need for deuterium labelling. At the air / water interface the adsorption isotherm was directly determined (70) in the concentration range  $2 \times 10^{-3}$  to  $0.2 \text{ g/L}$ , to indicate a critical aggregation concentration, CAC,  $\sim 3 \times 10^{-3} \text{ g/L}$  ( $\sim 0.4 \text{ \mu M}$ ), consistent with the observations of Cox et al (61). The mean area/molecule at saturation adsorption was  $420 \pm 20 \text{ \AA}^2$ , corresponding to an adsorbed amount of  $0.39 \pm 0.02 \times 10^{-10} \text{ mol cm}^{-2}$ . A densely packed monolayer with a thickness of  $31 \pm 2 \text{ \AA}$  and a volume fraction  $\sim 0.7$  was obtained, consistent with the general observations of Kisko et al (64). However there was no evidence of a more complex ordered structure at the air-water interface as implied in other studies (64-67). Zhang et al (70) showed that the surface adsorbed amount and thickness of the adsorbed HFB2 layer at the air / water interface was invariant with pH in the range 3 to 10 (HFB2 has an isoelectric point, IEP, of 3.5), indicating that the adsorption is dominated by the hydrophobic patch and not electrostatic interactions. At the solid / solution interface the structure of the adsorbed layer depended upon the nature of the solid surface, and neutron reflectivity was used to measure the hydrophobin adsorption at the hydrophilic



silica surface and a hydrophobic (OTS coated) surface. At the hydrophilic silica / water interface a thicker adsorbed layer,  $42 \pm 1 \text{ \AA}$ , with a volume fraction  $\sim 0.8$  was observed. Given the approximate molecular dimensions of the globular protein,  $24 \times 27 \times 30 \text{ \AA}$  (60), this implies the adsorption of a bilayer. It is probably in the form of dimers at the interface with the hydrophobic patch at the centre of the dimer, as reported in the crystal structure determination (60), and illustrated in figure 4b. This is also consistent with the more general observations for conventional surfactants which adsorb at the hydrophilic solid surface with a structure which reflects its bulk aggregation. At the hydrophobic solid surface (OTS coated) the OTS layer gives rise to a pronounced interference fringe in the data, which is further enhanced by the adsorption of the hydrophobin layer, see figure 5.

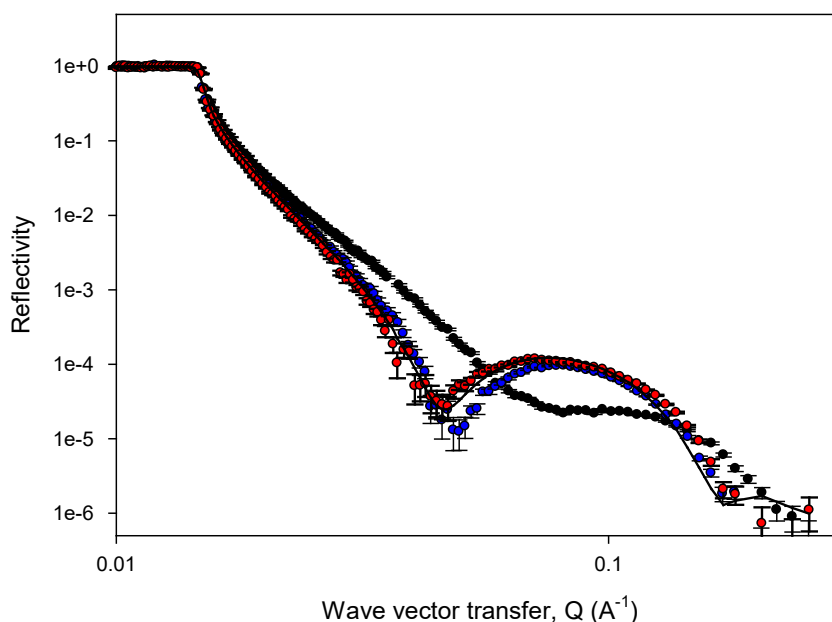


**Figure 5.** Neutron reflectivity data for hydrophobin adsorbed onto an OTS surface in  $D_2O$ ; (black) bare OTS surface, (red) + 0.2 mg/ml hydrophobin, (blue) after rinsing in  $D_2O$ . Reproduced from reference 71.

This is analysed as a thinner dense adsorbed layer, with a thickness  $\sim 20 \text{ \AA}$  and a volume fraction  $\sim 0.8$ . This suggests that the hydrophobin molecules are slightly tilted in their monolayer and bilayer structures at the solid surface, as shown in figure 4. This further suggests that the structure at the air-water interface contains some orientational and / or vertical disorder, associated with the slightly larger dimension and the lower packing

density. The other notable difference in the adsorption at the different solid surfaces is the strength of the binding observed. At the hydrophilic surface the binding between the hydrophilic groups of the hydrophobin to silica is relatively weak, and the hydrophobin can be readily removed by rinsing in water. This is similar to what is observed with conventional surfactants. At the hydrophobic surface there is a stronger attraction between the OTS layer and the hydrophobic patch on the hydrophobin, and the adsorbed layer is not readily removed by rinsing in water. As will be discussed in more detail later in the review it requires the use of a surfactant at concentrations  $\gg$  CMC to remove hydrophobin from the OTS surface.

### **4.3 Hydrophobin / surfactant adsorption**

As with many biosurfactants a key element in the wider exploitation of hydrophobin will be in the blending with other surface active proteins and conventional surfactants, and especially food grade surface active components. In the context of adsorption at interface there is an extensive literature on protein and protein / surfactant adsorption (22, 72-85), and some studies specifically on hydrophobin / surfactant (protein) adsorption (70, 71, 86-89) have been carried out.

The nature of the adsorption of protein / surfactant mixtures at interfaces will depend upon their interaction with each other in bulk and at the interface, and their relative surface activities. In that context the simplest interface to consider is the air / solution interface. It has been shown that broadly speaking the adsorption of protein / surfactant mixtures at the air / water interface resemble that associated with polyelectrolyte / surfactant mixtures (90, 91). That is, at low surfactant concentrations there is adsorption of both protein and surfactant which may be enhanced due to a favourable surface interaction between the surfactant and protein, and at higher surfactant concentrations the protein is displaced by the surfactant as the bulk protein / surfactant aggregation dominates over the surface interaction. This pattern of adsorption has been demonstrated in a number of studies using neutron reflectivity (22, 75, 76) and by other techniques, especially when it modifies the surface rheological properties (72-85). Zhang et al (70) used neutron reflectivity to study the adsorption of hydrophobin with a range of conventional surfactants, cetyltrimethyl ammonium bromide, CTAB, sodium dodecyl sulfate, SDS, and hexaethylene glycol monododecyl ether, C<sub>12</sub>E<sub>6</sub>, at the air / water interface. Measurements with and without the

conventional co-surfactant deuterium labelled enabled the amount of hydrophobin and surfactant at the interface to be directly determined. Figure 6 shows the variation in the amount of hydrophobin at the interface as a function of the cosurfactant concentration. The general trend that is observed is that below the surfactant CMC the surface adsorption is dominated by the hydrophobin, with an adsorbed amount close to its saturated value in the absence of cosurfactant. There is evidence that there is some co-adsorption of the surfactant in this region, and that it is more strong for SDS and CTAB in that order and less so for the nonionic surfactant. This implies that the surface interaction between hydrophobin and SDS is the strongest. At the cosurfactant CMC there is a marked decrease in the amount of hydrophobin at the interface for both CTAB and SDS, and the adsorption is now dominated by the co-surfactant. This implies that the bulk hydrophobin / surfactant aggregation in solution is now more energetically favourable than coadsorption.

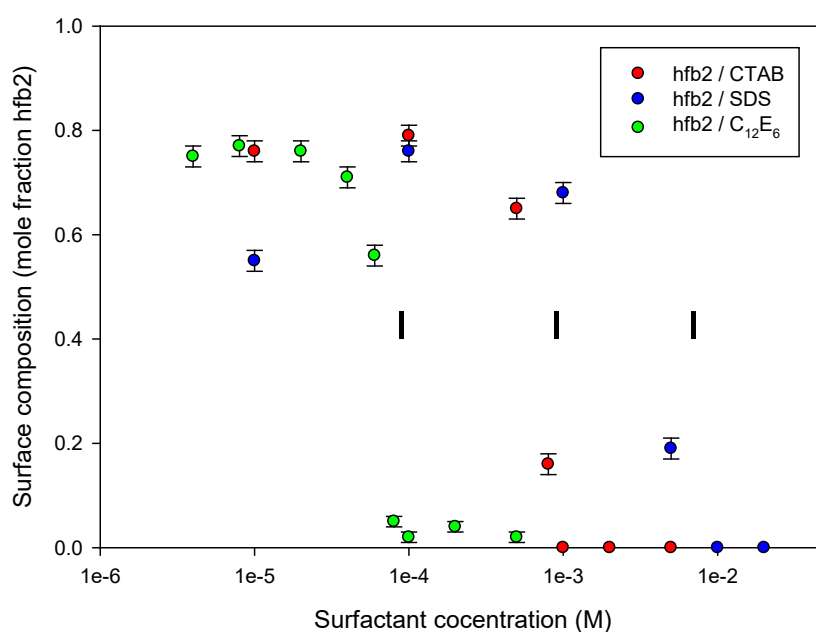


**Figure 6.** Variation in surface composition (mole fraction hydrophobin) for (red) hydrophobin / CTAB, (blue) hydrophobin / SDS and (green) hydrophobin / C<sub>12</sub>E<sub>6</sub>. The vertical tick marks indicate the pure surfactant cmc values. Reproduced from reference 70.

Although broadly similar, the pattern for hydrophobin / C<sub>12</sub>E<sub>6</sub> is slightly different, and at surfactant concentrations above the cmc for C<sub>12</sub>E<sub>6</sub> there is a measurable but small amount

of hydrophobin remaining at the interface. This implies that hydrophobin / C<sub>12</sub>E<sub>6</sub> complexation in bulk is less favourable. This is also observed at the interface where the amount of C<sub>12</sub>E<sub>6</sub> that co-adsorbs with hydrophobin is lower than for SDS and CTAB. The thickness of the adsorbed layer in the two different regions, as determined by the neutron reflectivity data, also reflect the change in the surface structure with then changing pattern of adsorption. For co-surfactant concentrations  $\ll$  CMC the thickness was  $\sim 36$  Å. This is slightly larger than that measured for hydrophobin alone,  $\sim 31$  Å, and reflects the change in packing to accommodate the coadsorption. Whereas above the cmc the thickness was  $\sim 20$  to  $24$  Å, consistent with the thickness expected for a CTAB or SDS monolayer (12). At lower pH, pH 3, the charge on the hydrophobin is reversed, as it is now below its IEP, and a stronger hydrophobin / SDS interaction occurs. It changes from a predominantly hydrophobic interaction to a charge mediated interaction. This results in the formation of a more complex layered structure at the interface, broadly similar to that observed in polyelectrolyte / surfactant mixtures (90, 91) and related systems (92). More complex layered structures were observed more extensively in a related hydrophobin / surfactant mixture, but driven by a different mechanism, and will be described and discussed in more detail later in the review.

#### **4.4 Hydrophobin / protein adsorption**

The size discrimination, as indicated in the neutron reflectivity structural measurements on the hydrophobin / surfactant mixtures, was exploited by Tucker et al (88) to probe hydrophobin / protein mixed adsorption at the air / water interface, in circumstance where deuterium labelling of either component was not possible. It was shown that the nature of the coadsorption depended upon the protein and the solution pH. It was observed that for the compact and tightly bound hydrophobin pH had little impact upon the adsorption at the air-water interface (70). For  $\beta$ -lactoglobulin the thickness of the adsorbed layer and its pH dependence implied partial disordering and denaturation at the interface, consistent with previous structural studies at the interface (76). However, the pH dependence is not substantial. For the more disordered protein,  $\beta$ -casein, the adsorption at the air / water interface is less compact and more diffuse in its extent, and also exhibits a more pronounced pH dependence. At pH 4 to 7 it comprises of two layers with a dense initial layer and a more diffuse outer layer, adjacent to the water phase. At pH 2.4 the adsorption

is in the form of a more compact single layer, consistent with previous observations. When  $\beta$ -lactoglobulin is mixed with hydrophobin the adsorption is completely dominated by the hydrophobin adsorption, and the  $\beta$ -lactoglobulin does not compete for the surface under any of the circumstances probed, and this is consistent with the observations of Wang et al (93). For  $\beta$ -casein / hydrophobin mixtures the surface properties were different and depended upon the relative concentration of the two components and the solution pH. At low pH, pH 2.4, like the hydrophobin /  $\beta$ -lactoglobulin mixture, the adsorption was dominated by the hydrophobin adsorption and little or no  $\beta$ -casein coadsorption was measureable. At higher pH the  $\beta$ -casein adsorbed and partially penetrated the hydrophobin layer at the interface to form a mixed layer, as illustrated in figure 7.

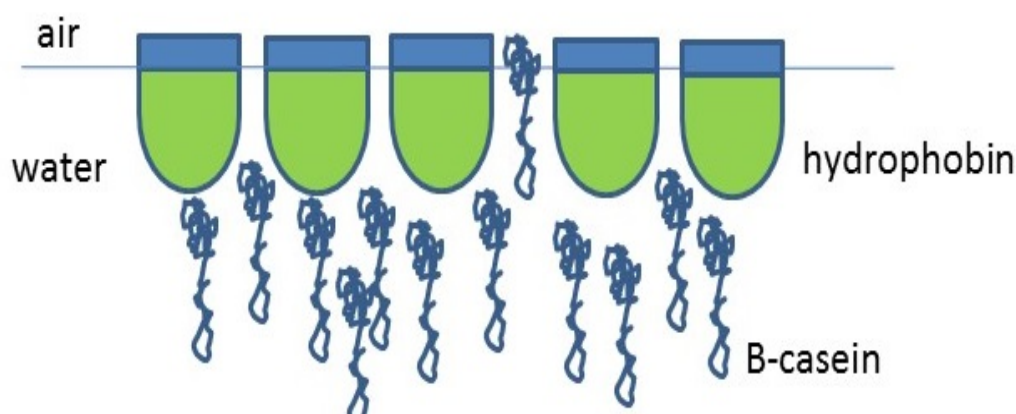


**Figure 7.** Schematic representation of the mixed hydrophobin /  $\beta$ -casein surface layer at high pH at the air-water interface; determined from neutron reflectivity data. Reproduced from reference 88.

The structure in figure 7, derived from the neutron reflectivity data, is consistent with the more indirect interpretation of surface rheology data by Radulova et al (87) and Wang et al (93).

At the solid / solution interface (71) the patterns of hydrophobin / surfactant adsorption follow broadly the trends observed at the air-water interface (70), but with differences that depend upon the nature of the interaction of both hydrophobin and surfactant with the solid surface. As discussed earlier, at the hydrophilic silica surface hydrophobin adsorbs reversibly in the form of a bilayer, and hydrophobin dominates the adsorption in mixtures

with CTAB and SDS below the cosurfactant CMC. Above the CMC the CTAB replaces the hydrophobin at the interface; whereas for SDS there is no adsorption of either hydrophobin nor SDS at the interface. A similar range of measurements were made for mixtures of hydrophobin with CTAB, SDS and  $C_{12}E_6$  at the hydrophobic solid surface, in which the hydrophobic nature of the surface was established using an OTS layer, see earlier discussion. At the hydrophobic surface the hydrophobin is irreversibly adsorbed such that rinsing in solvent or in a surfactant solution, SDS or CTAB, below the CMC has no impact upon the adsorption. However above the CMC the SDS or CTAB removes entirely the hydrophobin from the surface. For the nonionic surfactant,  $C_{12}E_6$ , some coadsorption between the  $C_{12}E_6$  and hydrophobin takes place, but otherwise the  $C_{12}E_6$  has little impact upon the hydrophobin adsorption below or above the CMC. These results clearly indicate that not only is the nature of the interaction of hydrophobin and surfactant with the interface important but also that the nature of the interaction between surfactant and hydrophobin can profoundly change the surface interaction.

#### **4.5. Hydrophobin / Tween surface layering**

Finally Tucker et al (89) used neutron reflectivity to explore the adsorption of hydrophobin and  $\beta$ -casein mixtures at the hydrophilic solid / liquid interface. Measurements were made to explore both sequential and coadsorption, and the interpretation of the data relied upon the size discrimination between the hydrophobin and the  $\beta$ -casein.  $\beta$ -casein adsorbed onto the hydrophilic silica surface with a layer  $\sim 55$  Å in thickness and with a volume fraction at saturation adsorption  $\sim 0.4$ . Adsorption of  $\beta$ -casein onto a pre-adsorbed hydrophobin layer resulted in the hydrophobin being largely displaced by the  $\beta$ -casein for  $\beta$ -casein concentrations  $\geq 0.1$  wt %; displaying a competitive adsorption action similar to that observed with conventional surfactants. In the co-adsorption measurements the adsorption is dominated by the  $\beta$ -casein and indicates a greater affinity of the  $\beta$ -casein for the surface compared to hydrophobin. The differences compared to the air / water interface further reinforce the importance of the interaction with the solid surface in determining the adsorption behaviour.

The earlier studies using neutron reflectivity on the mixture of ionic and nonionic surfactants with hydrophobin (69, 70) highlighted the nature of competitive adsorption and provided some indication that specific interactions may result in more complex surface

interactions and surface structures. This was further explored by Tucker and coworkers (94, 95) using neutron reflectivity to investigate the surface adsorption of hydrophobin with a range of Tween-like nonionic surfactants. The interaction of nonionic surfactants with proteins is particularly important as the interaction is weak and this minimises the effects of denaturation and promotes other properties associated with solubilisation, suppression of aggregation and adsorption (96). The Tween surfactants are ethoxylated polysorbates, and are an important class of food grade surfactants. They are used extensively in emulsion and foam stabilisation (96, 97), and so are important in the context of potential applications of hydrophobin. The Tween surfactants are comprised of ethoxylated sorbitan esters linked to a range of different fatty acids. The commercially available Tweens mostly have twenty ethylene oxide groups attached to the sorbitan group to form the hydrophilic headgroup. The headgroup is attached to a single long chain carboxylic acid, lauric, palmitic, stearic or oleic; named Tween 20, 40, 60 or 80, and the structure of Tween 20 is shown in figure 8.

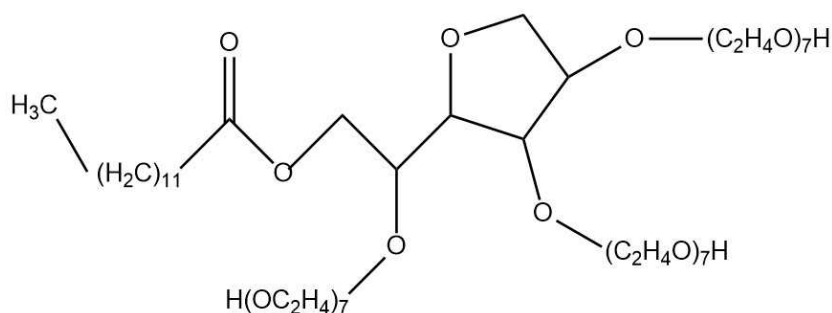
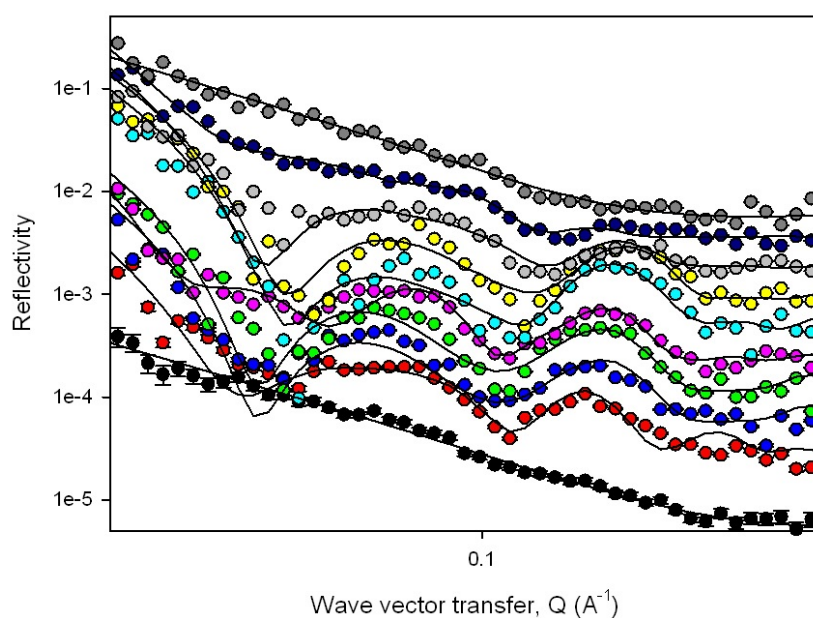


**Figure 8.** Molecular structure of the Tween 20 surfactant.

In addition to their extensive use in foam and emulsion stabilisation (96, 97) they have been used to suppress protein aggregation and promote protein refolding in recombinant systems (98). Their competitive adsorption properties with a range of other proteins has been explored (79, 99, 100).

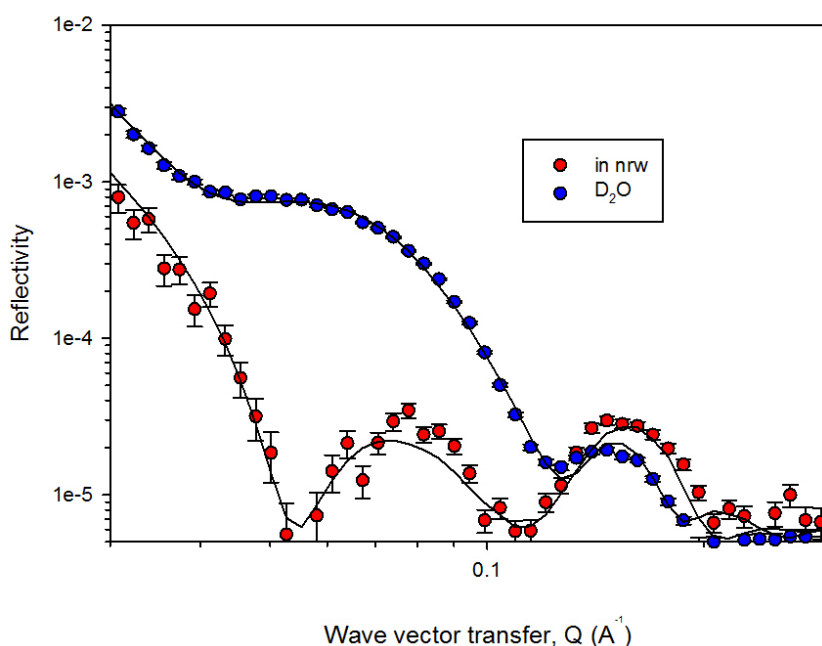
To investigate the nature of hydrophobin / Tween adsorption Tucker and coworkers (94, 95) custom synthesised a range of Tween-like surfactants with lauric, palmitic, stearic and oleic alkyl chains, and degrees of ethoxylation of the sorbitan headgroup which ranged from three to twenty. The surfactants were synthesised with the ethylene oxide groups deuterium labelled or hydrogenous, where the deuterium labelled versions provide a good neutron contrast to the hydrophobin. The surfactants are abbreviated as PES<sub>n</sub>-20, 40, 60 or

80, where 20, 40, 60 and 80 refer to the lauric, palmitic stearic or oleic alkyl chain, and  $n$  is the degree of ethoxylation. The adsorption properties the PES Tween-like surfactants were fully characterised by neutron reflectivity (101). For a given degree of ethoxylation the adsorption isotherms are largely independent of the alkyl chain length (93), whereas for a fixed alkyl chain length the area / molecule depends linearly upon the degree of ethoxylation (101). The neutron reflectivity measurements for the deuterium labelled PES<sub>8</sub>-60 /hydrophobin mixture at the air-water interface at different surfactant concentrations and a fixed hydrophobin concentration showed a remarkable and unexpected evolution in the structure of the adsorbed layer (94), as shown in figure 9a.



(a)





(b)

**Figure 9.** (a) Neutron reflectivity data for PES<sub>8</sub>-60 /0.05 mg/ml hydrophobin in nrw: (from bottom to top) (black) 1000  $\mu$ M PES<sub>8</sub>-60, (red) 500, (blue) 275, (green) 165, (pink) 100, (cyan) 50, (yellow) 25, (grey) 12.5, (dark blue) 6.25, (dark grey) 3.1. The different curves are shifted vertically for clarity. (b) Neutron reflectivity data for 50  $\mu$ M PES<sub>8</sub>-60 / 0.05 mg/ml hydrophobin in nrw (red) and in D<sub>2</sub>O (blue). The solid lines are model fits for the model shown in figure 10 and described in detail elsewhere (94). The figures are reproduced from reference 94.

At the highest PES<sub>8</sub>-60 concentration, 1000  $\mu$ M, the reflectivity data are from a monolayer dominated by the surfactant adsorption, with an area / molecule,  $\sim 75 \text{ \AA}^2$  and thickness,  $\sim 20 \text{ \AA}$ , consistent with a saturated monolayer of surfactant. At the other extreme of surfactant concentration, 3.1  $\mu$ M, the reflectivity is again in the form of a monolayer with a thickness  $\sim 30 \text{ \AA}$ , and consistent with the surface now being dominated by the hydrophobin adsorption. At the intermediate surfactant concentrations the reflectivity and surface structure is more complex. The reflectivity is now best described a two interference fringes which are most well defined and prominent in the middle of the surfactant concentration range explored and less so at the extremes close to the transitions to a pure surfactant or hydrophobin monolayer. Further measurements, in which the solvent contrast is changed

from nrw to D<sub>2</sub>O, show a consistent pattern, see figure 9b, and provides additional constraints in the modelling. The simplest model consistent with all the data is shown in figure 10.

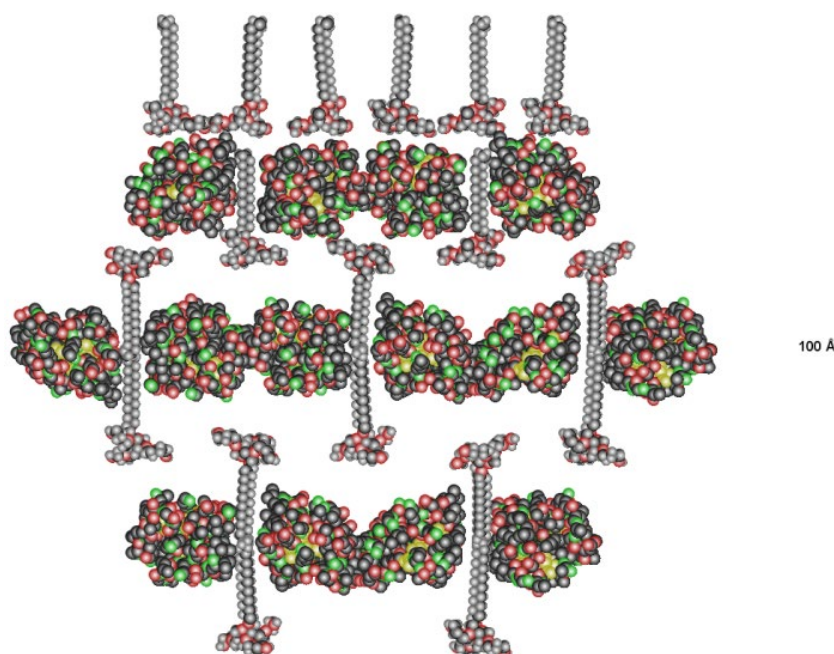
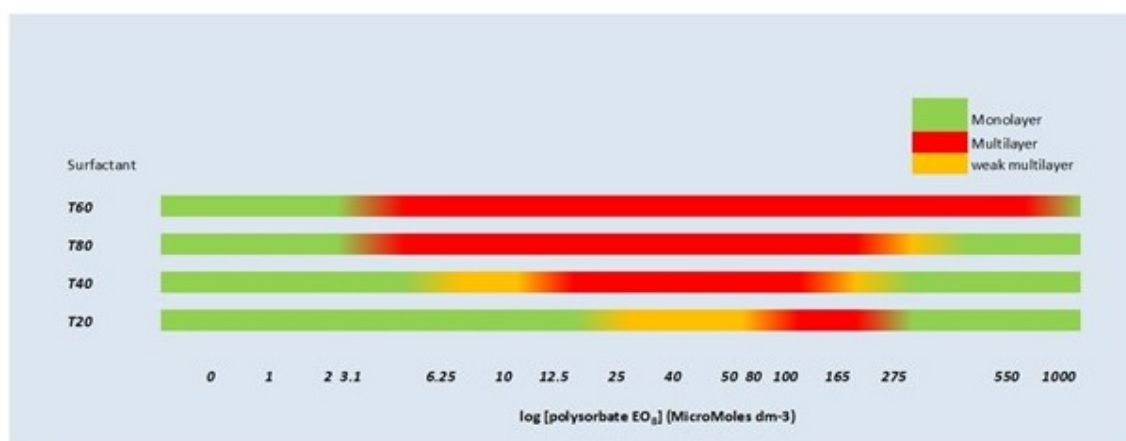


**Figure 10.** Schematic representation of the PES8-60 / hydrophobin surface structure, derived from the modelling of the neutron reflectivity data in figure 9. The figure is reproduced from reference 94.

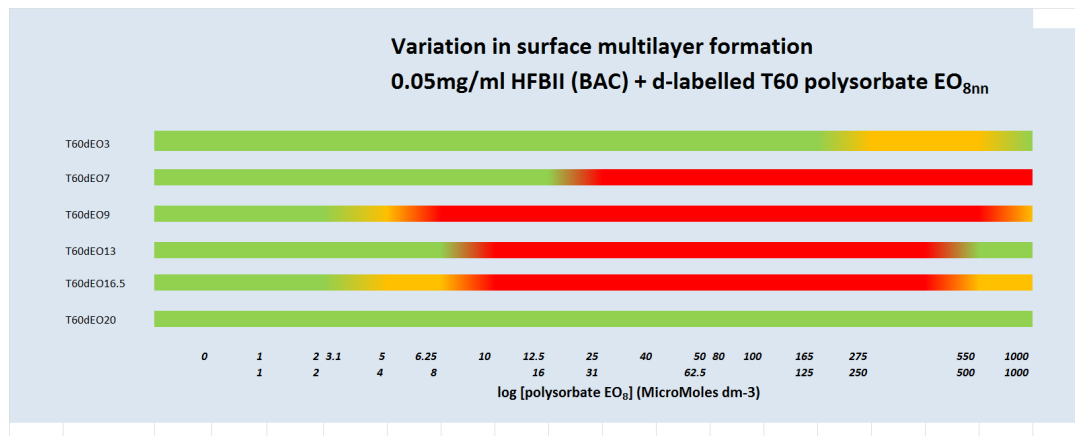
The model is best characterised by six layers, with an initial monolayer adjacent to the air phase,  $\sim 15$  to  $20$  Å, of deuterated surfactant, followed by layers of hydrophobin,  $\sim 30$  Å, separated by thin layers,  $10$  to  $15$  Å, that contain mainly the deuterated ethoxylated polysorbate headgroups. At the extremes of the concentration range the structures are less well defined and developed due to vertical and lateral disorder, and can sometimes be described by a smaller number of layers. Although there is some variation in the structure, the general model fits a wide range of equivalent data (94, 95) in which the surfactant type and the relative concentrations of the surfactant and hydrophobin are varied.

If the adjacent ethoxylated polysorbate and hydrophobin layers are considered as a pair, then the structure comprising the six layers can be thought of as three bilayers. In that case the interference fringe at high  $Q$ ,  $\sim 0.15$  Å<sup>-1</sup>, is a Bragg peak broadened by the small number

of bilayers, and the interference fringe at lower  $Q$ ,  $\sim 0.08 \text{ \AA}^{-1}$ , relates to the total thickness of the layer. Similar structures and structural evolutions were reported for the PES surfactants with the same degree of ethoxylation in the headgroup but with differing alkyl chain lengths and geometries. The approximate surface phase diagram for PES<sub>8</sub>-20, 40, 60, and 80 are shown on figure 11a.



(a)



(b)

**Figure 11.** (a) Surface phase diagram for 0.05 mg/ml hydrophobin and PES<sub>8</sub>-20,40,60,80, see legend for details (b) Surface phase diagram for 0.05 mg/ml hydrophobin and PES<sub>n</sub>-60 with  $n=3, 7, 9, 13, 16.5, 20$ , see legend for details. Reproduced from references 94 and 95.

Figure 11b shows how the surface structure varies for PES<sub>n</sub>-60 / hydrophobin mixtures as the degree of ethoxylation,  $n$ , of the surfactant is varied. Importantly it illustrates that at the extremes of ethoxylation, 3 and 20, there is almost no surface ordering observed, and this

has important implications for the factors which are driving this unusual surface structure. Indeed the commercially available Tweens, with a degree of ethoxylation of twenty, it is unlikely that the surface layering would have been revealed.

The structure deduced from the data, figure 10, provides some insights into the factors and interactions that are driving the formation of the layered structure. The structure implies that the formation of the layered structure results from the hydrophobic interaction between the polysorbate alkyl chains and the hydrophobic patches on the hydrophobin surface, and the interaction between the ethoxylated sorbitan headgroup and the hydrophilic regions of the hydrophobin. The structure can be described as a 'bricks and mortar' structure, where the hydrophobin represents the 'bricks' and the surfactant the 'mortar'; in which the ethoxylated polysorbate headgroups are the mortar between the horizontal layers and the alkyl chains the 'mortar' in the vertical gaps between what are essentially hydrophobin dimers. In this respect the stearate alkyl chain,  $\sim 22$  Å, appears to be the most optimal for the packing with the hydrophobin, and the lauric and palmitic chains,  $\sim 17$  and  $20$  Å respectively, are less optimal. The oleic chain is also not as optimal as the stearic, which is most likely associated with the less favourable packing of the unsaturated alkyl chains. The variation of the surface ordering with the degree of ethoxylation also provides some insight into the role of the ethoxylated polysorbate headgroup. Estimates of the relative packing of the surfactant and hydrophobin layers (95) indicate that in the range of degrees of ethoxylation from 9 to 12 the ratio of surfactant / hydrophobin in the layers varies from 3.5 to 5 where the optimal layering occurs. This suggests that at the extremes of the degrees of ethoxylation, 3 and 20, the packing requirements for the surfactant, PES<sub>3</sub>-60 and PES<sub>20</sub>-60 have area / molecule of 37 and 125 Å<sup>2</sup> respectively, are too small or too large to accommodate the optimal packing required for the hydrophobic and hydrophilic interactions required to stabilise the layered structure.

The specific nature of the interactions that promote the layered structures and the packing requirements associated with the PES structure are highlighted when comparison is made with other related systems. It was found that a broadly analogous nonionic surfactant, decaethylene monstearyl ether, C<sub>18</sub>E<sub>10</sub>, did not form layered structures with hydrophobin (95). Furthermore the coadsorption of PES<sub>n</sub>-60 with a range of other proteins with different

structures, which included  $\beta$ -lactoglobulin,  $\beta$ -casein, and lysozyme, also showed no evidence of surface ordering (94).

Finally it is important to note that the formation of the layered surfactant / hydrophobin structures at interfaces results in some different wetting properties. It has been previously reported by Graca et al (102) that the adsorption of the Tween surfactants onto hydrophobic surfaces forms robust layers which have potential applications for lubrication. Prime et al (103) demonstrated the importance of ethoxylated surfaces in inhibiting non-specific adsorption of proteins. The adsorption of the ethoxylated polysorbate / hydrophobin mixtures offer some different wetting opportunities. It was shown that hydrophobin strongly adsorbs to form hydrophobic surfaces, and is the origin of much of its biofunctionality (6, 66, 67). Whereas the adsorption of hydrophobin strongly wets hydrophobic surfaces, the adsorption of the layered ethoxylated polysorbate / hydrophobin films results in a surface that remains highly hydrophobic. This is in contrast to the wetting properties associated with the adsorption of multilayer structures found in ionic surfactants mixed with multivalent ions and polyions (90-92), which persistently wet hydrophobic surfaces. These differences arise from the differences in the respective surface structures and the different mechanisms associated with their formation. Hence the ethoxylated polysorbate / hydrophobin mixtures offer new opportunities for the manipulation of surface properties for a range of home and personal care products, cosmetics, pharmaceuticals, food products (104) and in biomedical (105) and biotechnological (106) applications.

## **5. SUMMARY and FUTURE PROSPECTS**

This review has focussed on the adsorption of two specific biosurfactants which are attracting much current interest, the glycoside saponin, and the fungal protein hydrophobin. The emphasis has been on the role of neutron reflectivity in investigating the surface adsorption and the structure of the adsorbed layer. The important breakthrough is that because of the development of neutron sources and associated instrumentation and because the elemental composition of such biosurfactants deuterium labelling is not an overriding requirement.

The results presented have provided some important insights into the adsorption properties of both of the biosurfactants studied that were not accessible using other techniques. It

offers great potential for the study of a wider variety of biosystems. The importance of a well-defined system with an acceptable level of purity is however highlighted, and this will be a limiting factor in the systematic study of some systems. Furthermore it has been demonstrated how other surface techniques can provide important complementary information, which combined with the neutron reflectivity data can result in an even greater understanding.

Finally there is great potential for the study of mixed systems which incorporate such biosurfactants, especially when the co-surfactant can be deuterium labelled. The progress in studying saponin mixed with surfactants and proteins using neutron reflectivity has so far been limited. However the review, through the studies on hydrophobin / surfactant and hydrophobin / protein adsorption, demonstrates the power of neutron reflectivity to probe adsorption and mixed adsorption in such systems. The study of mixed adsorption remains an area of great potential, and is crucially linked to the potential wider application of biosurfactants in many of the product sectors.

## REFERENCES

- (1) Holmberg K. Natural surfactants. *Curr. Opin. Coll. Int. Sci.* 2001; 6: 148-159
- (2) Foley P. Kermanshahi Pour A. Beach ES. Zimmerman JB. Derivation and synthesis of renewable surfactants. *Chem. Soc. Rev.* 2012; 41: 1499-1518
- (3) Otzen DE. Biosurfactants and surfactants interacting with membranes and proteins. *Biochimica et Biophysica Acta.* 2017; 1859: 639-649
- (4) Roz EZ. Rosenberg E. Natural role of biosurfactants. *Environ. Microbiol.* 2001; 3: 229-236
- (5) Gulu-Ustundag O. Mazza G. Saponin: properties, applications and processing. *Crit. Rev. in Food Science and Nutrition.* 2007; 47: 231-258
- (6) Linder MB. Hydrophobins: proteins that self-assemble at interfaces. *Curr. Opin. Coll. Int. Sci.* 2009; 14: 356-363
- (7) Raaijmakers JM. deBriujn I. Nybroe O. Ungena M. Natural function of lipopeptides from *Bacillus* and *Pseudomonas*: more than surfactants and antibiotics. *FEMS Microbiol. Rev.* 2010; 34: 1037-1062
- (8) Georgiou G. Lin SC. Sharma MM, Surface active compounds from bio-organisms, *Biotechnol.* 1992; 10: 60-65
- (9) Desai JD. Banat IM. Microbial production of surfactants and their commercial potential. *Microbiol. Mol. Biol. Rev.* 1997; 61: 47-64
- (10) Karanth NGK. Deo PG. Keenanudig NK. Microbiological production of biosurfactants and their importance. *Curr. Sci.* 1999; 77: 116-126
- (11) Kosaric M. Biosurfactants in industry. *Pure Appl. Chem.* 1992; 64: 1731-1737
- (12) Lu JR. Thomas RK. Penfold J. Surfactant layers at the air-water interface: structure and composition. *Adv. Coll. Int. Sci.* 2000; 85: 143-304
- (13) Penfold J. Thomas RK. Mixed surfactants at the air-water interface, *RSC Annual Rep. Prog. Chem. section C.* 2010; 106: 14-35
- (14) Penfold J. Thomas RK. Shen HH. Adsorption and self-assembly of biosurfactants studied by neutron reflectivity and small angle neutron scattering: glycolipids, lipopeptides and proteins. *Soft Matter.* 2012; 8: 578-591
- (15) Chen ML. Penfold J. Thomas RK. Smythe TJP. Perfumo A. Marchant R. Banat IM. Stevenson PS. Parry A. Tucker I. Grillo I. Solution self-assembly and adsorption at

- the air-water interface of the mono and dirhamnolipids and their mixtures. *Langmuir*. 2010; 26: 18281-18292
- (16) Chen ML. Penfold J. Thomas RK. Smythe TJP. Perfumo A. Marchant R. Banat IM. Stevenson PS. Parry A. Tucker I. Grillo I. Mixing behaviour of the biosurfactant rhamnolipid with a conventional anionic surfactant, sodium dodecyl benzene sulfonate. *Langmuir*. 2010; 26: 17958-17968
- (17) Chen ML. Dong CC. Penfold J. Thomas RK. Smythe TJP. Perfumo A. Marchant R. Banat IM. Stevenson PS. Parry A. Tucker I. Grillo I. The influence of calcium ions on rhamnolipid and rhamnolipid / anionic surfactant adsorption and self-assembly. *Langmuir*. 2013; 29: 3912-3923
- (18) Liley J. Penfold J. Thomas RK. Tucker IM. Petkov JT. Stevenson PS. Banat IM. Marchant R. Rudden M. Webster JRP. Adsorption at the air-water interface in biosurfactant-surfactant mixtures: quantitative analysis of adsorption of a five-component mixture. *Langmuir*. 2017; 33: 13027-13039
- (19) Chen ML. Penfold J. Thomas RK. Smythe TJP. Perfumo A. Marchant R. Banat IM. Stevenson PS. Parry A. Tucker I. Campbell RA. Adsorption of sophorolipid biosurfactants on their own and mixed with sodium dodecyl benzene sulfonate at the air-water interface. *Langmuir*. 2011; 27: 8854-8866
- (20) Shen HH. Thomas RK. Penfold J. Fragneto G. Destruction and solubilisation of supported phospholipid bilayers on silica by the biosurfactant surfactin. *Langmuir*. 2010; 26: 7334-7342
- (21) Shen HH. Thomas RK. Chen CY. Darkin RC. Baker SC. Penfold J. The aggregation of the naturally occurring lipopeptide surfactin at interfaces and in solution: an unusual type of surfactant. *Langmuir*. 2009; 25: 4211-4218
- (22) Lu JR. Zhao X. Yaseen M. Protein adsorption studied by neutron reflectivity, *Curr. Opin. Coll. Int. Sci.* 2007; 12: 9-16
- (23) Su TJ. Lu JR. Thomas RK. Cui ZF. Penfold J. The conformational structure of BSA layers adsorbed at the silica-water interface. *J. Phys. Chem. B*. 1998; 102: 8100-8108
- (24) Su TJ. Lu JR. Thomas RK. Cui ZF. Penfold J. The effect of solution pH on the structure of Lysozyme layers adsorbed at the silica-water interface studied by neutron reflectivity. *Langmuir*. 1998; 14: 438-445



- (25) Lu JR. Su TJ. Penfold J. Adsorption of serum albumins at the air-water interface. *Langmuir*. 1999; 15: 6975-6983
- (26) Born M. Wolf E. Principles of optics. Pergammon; 1970
- (27) Heavens OS. Optical properties of thin films. Dover; 1955
- (28) Penfold J. Thomas RK. The application of specular neutron reflection to the study of surfaces and interfaces. *J. Phys. Condens. Matt*. 1990; 2: 1369
- (29) Lekner J. Theory of reflection. Martinus Nijhoff; 1987
- (30) Guglu-Ustundag O. Mazza G. Saponins: properties, applications and processing. *Crit. Rev. in Food Science and Medicine*. 2007; 47: 231-258
- (31) Vincken JP. Heng L. de Groot A. Gruppen H. Saponins: classification and occurrence in the plant kingdom. *Phytochemistry*. 2007; 68: 275-297
- (32) Sparg SG. Light ME. van Studen J. Biological activities and distribution of plant species. *J. Ethno-pharmacology*. 2004; 94: 219-243
- (33) Oakenfull D. Saponins in food: a review. *Food Chemistry*. 1981; 6: 19-40
- (34) Hoslettmann K. Marstom A. Saponins. Cambridge University Press; 1995
- (35) Cheeke PR. Actual and potential application of Yucca Schidigera and Quillaja Saponana saponins in human and animal nutrition. *Proc. Am. Soc. Anim. Sci*. 1999;; E9: 1-10
- (36) Jenkin KJ. Atwall AS. Effects of dietary saponins in fecal bile acids and neutral steroids and availability of vitamin A and E in the chick. *J. Nutr. Biochem*. 1994; 5: 134-137
- (37) Brown R. The natural way in cosmetics and skin care, *Chem. Mark. Rep*. 1998; 254: FR8
- (38) Liu J. Henkel T. Traditional Chinese medicine (TCD): are polyphenols and saponins key ingredients triggering biological activity. *Curr. Med. Chem*. 2002; 9: 1483-1485
- (39) Fukuda N. Tanaka H. Shoyama Y. Isolation of the pharmacological active saponin, Ginzenoside Rb1 from Ginseng by immunoaffinity column chromatography. *J. Nat. Prod*. 2000; 62: 283-285
- (40) Sirtori CR. Aescin: pharmacology, Pharmokinetics and therapeutic profile. *Pharmacol. Res*, 2001; 44: 183-193

- (41) Pagureva N. Tcholakova S. Golemanov K. Denkov N. Pelan E. Stoyanov S. Surface properties of adsorption layers formed from triperpenoid and steroid saponins. *Coll. Surf. A*. 2016; 491: 18-28
- (42) Stanimorova R. Marinova K. Tcholakova S. Denkov N. Stoyanov S. Pelan, E. Surface rheology of saponin adsorption layers. *Langmuir*. 201; 27: 12486-12498
- (43) Wojciechowski K. Surface activity of saponins from Quillaja Bark at the air/water and oil/water interfaces. *Coll. Surf. B*. 2019; 108: 95-107
- (44) Golemanov K. Tcholakova S. Denkov N. Pelan E. Stoyanov S. Surface shear rheology of saponin adsorption layers. *Langmuir*. 2012; 28: 12071-12084
- (45) Golemanov K. Tcholakova S. Denkov N. Pelan E. Stoyanov S. Remarkably high surface viscoelasticity of adsorption layers of triterpenoid saponins. *Soft Matter*. 2013; 9: 5738-5752
- (46) Tsibranska S. Ivanova A. Tcholakova S. Denkov N. Self-assembly of Escin molecules at the air-water interface as studied by molecular dynamics. *Langmuir*. 2017; 33: 8330-8341
- (47) Penfold J. Thomas RK. Tucker I. Petkov JT. Stoyanov SD. Denkov N. Golemanov K. Tcholakova S. Webster JRP. Saponin adsorption at the air-water interface- neutron reflectivity and surface tension studies. *Langmuir*. 2018; 34: 9540-9547
- (48) Wojciechowski K. Orczyk M. Marcinkowski K. Kobiela T. Trupp M. Gutberlet T. Geue T. Effect of hydration of sugar groups on adsorption of Quillaja Bark saponin at air-water and silica – water interfaces. *Coll. Surf. B*. 2014; 117: 60-67
- (49) Wojciechowski K. Orczyk M. Gutberlet T. Geue T. Complexation of phospholipids by triterpenic saponins in bulk and in monolayers, *Biochimica et Biophysica Acta*. 2016; 1858: 363-373
- (50) Wojciechowski K. Orczyk M. Gutberlet T. Geue T. Complexation of phospholipids and cholesterol by triterpenic saponins in bulk and in monolayers. *Biochem. Biophys. Acta. Biomembr.* 2016; 1858: 363-373
- (51) Mitra S. Dungan S. Micellar properties of Quillaja saponin, 1. Effects of temperature, salt and pH on solution properties. *J. Agric. Food Chem.* 1997; 45: 1587-1595

- (52) Oakenfull DG. Aggregation of saponin and bile salts in aqueous solution. Aust. J. Chem. 1986; 39: 1671-1683
- (53) Jian HL. Liao XX. Zhu LW. Zhang WM. Jiang JX. Synergism and foaming properties in binary mixtures of a biosurfactant derived from *Camellia oleifera* Able and synthetic surfactants. J. Coll. Int. Sci. 2011; 359: 487-492
- (54) Kezwon A. Wojciechowski K. Interaction of Quillaja Bark saponins with food related surfactants. Adv. Coll. Int. Sci. 2014; 209: 185-195
- (55) Piotrowski M. Lewandowska J. Wojciechowski K. Biosurfactant- protein mixtures: Quillaja Bark saponin at the water-air and water-oil interfaces in the presence of  $\beta$ -lactoglobulin. J. Phys. Chem. B. 2012; 116: 4843-4850
- (56) Reichart CL. Salminen H. Bonisch CB. Schaefer C. Weiss J. Concentration effect of Quillaja saponin- cosurfactant mixtures on emulsifying properties. J. Coll. Int. Sci. 2018; 519: 71-80
- (57) Wojciechowski K. Pitrowski M. Popidarz W. Sosonowski TR. Short and mid-term adsorption behaviour of Quillaja Bark saponin and its mixtures with Lysozyme. Food Hydrocolloids. 2011; 25: 687-693
- (58) Linder MB. Hydrophobins: proteins that self-assemble at interfaces. Curr. Opin. Coll. Int. Sci. 2009; 14: 356-363
- (59) Hakaupaa J. Szilvay GR. Kaljunen H. Maksimainen M. Linder M. Rouvienen J. Two crystal structure of *Trichoderma reesi* hydrophobin HFB1 - structure of a protein amphiphile with and without detergent interactions. J. Protein Sci. 2006; 15: 2129-2140
- (60) Kallio JM. Linder MB. Rouvienen J. Crystal structures of hydrophobin HFB11 in the presence of detergent implicate the formation of fibril and monolayer films. J. Biol. Chem. 2007; 282: 28733-28739
- (61) Cox AR. Cagnol F. Russell AB. Izzard MJ. Surface properties of class II hydrophobins from *Trichoderma reesi* and the influence on bubble stability. Langmuir. 2007; 23: 7995-8002
- (62) Walther A. Muller AEH. Janus particles. Soft Matter. 2009; 4: 663-668
- (63) Cox AR. Aldred DL. Russell AB. Exceptional stability of food foams using class II hydrophobin, HFB2. Food Hydrocolloids. 2009; 23: 366-376

- (64) Kisko K. Szilvay GR. Vuorimaa E. Lemmetyinen H. Linder MB. Torkeli M. Serima R. Self-assembled films of hydrophobin HFB1 and HFB2 studied in-situ at the air-water interface. *Langmuir*. 2009; 25: 1612-1619
- (65) Lumsdon SO. Green J. Stieglitz B. Adsorption of hydrophobin proteins at hydrophobic and hydrophilic interfaces. *Coll. Surf. B*. 2005; 44: 172-178
- (66) Szilvay GR. Paananen A. Laurikainen K. Vuorimaa E. Lemmetyinen H. Peltonen J. Linder MB. Self-assembled hydrophobin films at the air-water interface: structural analysis and molecular engineering. *Biochem*. 2007; 46: 2345-2354
- (67) Wosten HAB. Schuren FHJ. Wessels JGH. Interfacial self-assembly of a hydrophobin onto an amphiphilic membrane mediates fungal attachment to hydrophobic surfaces. *The EMBO Journal*. 1994; 13: 5848-5854
- (68) Kisko K. Szilvay GR. Vainio U. Linder MB. Serima R. Interactions of hydrophobin proteins in solutions studied by small angle x-ray scattering. *Biophys. J*. 2008; 94: 198-206
- (69) Zhang XL. Penfold J. Thomas RK. Tucker IM. Petkov JT. Bent J. Cox A. Grillo I. Self-assembly of hydrophobin and hydrophobin / surfactant mixtures in aqueous solution. *Langmuir*. 2011; 27: 10514-10522
- (70) Zhang XL. Penfold J. Thomas RK. Tucker IM. Petkov JT. Bent J. Cox A. Campbell RA. Adsorption behaviour of hydrophobin and hydrophobin / surfactant mixtures at the air-water interface. *Langmuir*. 2011; 27: 11316-11323
- (71) Zhang XL. Penfold J. Thomas RK. Tucker IM. Petkov JT. Bent J. Cox A. Adsorption behaviour of hydrophobin and hydrophobin / surfactant mixtures at the solid-solution interface. *Langmuir*. 2011; 27: 10464-10474
- (72) Dickinson E. Adsorbed protein layers at fluid interfaces: interactions, structure and surface rheology. *Coll. Surf. B*. 1999; 15: 161-176
- (73) Murray BS. Rheological properties of protein films. *Curr. Opin. Coll. Int. Sci*. 2011; 16: 27-35
- (74) Wierenga PA. Gruppen H. New view on foams from protein films. *Curr. Opin. Coll. Int. Sci*. 2010; 15: 365-373
- (75) Green RJ. Su TJ. Joy H. Lu JR. Interaction of Lysozyme and SDS at the air-liquid interface. *Langmuir*. 2000; 16: 5797-5805

- (76) Horne DS. Atkinson PJ. Dickinson E. Pinfield VJ. Richardson RM. Neutron reflectivity study of competitive adsorption of  $\beta$ -lactoglobulin and nonionic surfactant at the air-water interface. *Int. Dairy J.* 1998; 8: 73-77
- (77) Kotsmar CS. Kragel J. Kovalchuk VI. Aksenkov EV. Fainerman VB. Miller R. Dilation and shear rheology of mixed  $\beta$ -casein / surfactant adsorption layers. *J. Phys. Chem. B.* 2009; 113: 103-113
- (78) Kotsmar CS. Grigoriev DO. Xu F. Aksenkov EV. Fainerman VB. Leser ME. Miller R. Equilibrium adsorption of mixed milk protein / surfactant solutions at the air / water interface. *Langmuir.* 2008; 24: 13977-13984
- (79) Kragel J. Wustneck R. Hushand F. Wilde PJ. Makievski AV. Grigoriev DO. Li JB. Properties of mixed protein / surfactant adsorption layers. *Coll. Surf. B.* 1999; 12: 399-407
- (80) Mackie AR. Gunning AP. Ridout MJ. Wilde PJ. Patino JR. In-situ measurements of the displacement of protein films from the air-water interface by surfactants. *Biomacromol.* 2001; 2: 1001-1006
- (81) Mackie AR. Gunning AP. Ridout MJ. Wilde PJ. Morris VJ. Orogenic displacement on mixed  $\beta$ -lactoglobulin /  $\beta$ -casein films at the air-water interface. *Langmuir.* 2001; 17: 6593-6598
- (82) Woodward NC. Gunning AP. Mackie AR. Wilde PJ. Morris VJ. Comparison of orogenic displacement of sodium caseinate with the caseins at the air-water interface by nonionic surfactants. *Langmuir.* 2009; 25: 6739-6744
- (83) Valderrama JM. Patino JMR. Interfacial rheology in protein / surfactant mixtures. *Curr. Opin. Coll. Int. Sci.* 2010; 15: 271-282
- (84) Valderrama JM. Molina AM. Rodriguez AM. Cabrerizo-Valchez MA. Galvez-Ruiz MJ. Langevin D. Surface properties and foam stability of protein/ surfactant mixtures: theory and experiment. *J. Phys. Chem. C.* 2007; 111: 2715-2723
- (85) Miller R. Alahverdijeva VS. Fainerman VB. Thermodynamics and rheology of mixed protein-surfactant adsorption layers. *Soft Matter.* 2008; 4: 1141-1146
- (86) Burke J. Cox A. Petkov J. Murray BS. Interfacial rheology and stability of air bubbles stabilised by mixtures of hydrophobin and  $\beta$ -casein. *Food Hydrocolloids,* 2014; 34: 119-127

- (87) Radulova GM. Golemanov. K. Danov KD. Kralchevsky PA. Stoyanov SD. Arnaudov LN. Blijdenstein TBJ. Pelan EG. Lips A. Surface shear rheology of adsorption layers from the protein HFB2 hydrophobin: effect of added  $\beta$ -casein. *Langmuir*. 2012; 28: 4168-4177
- (88) Tucker IM. Petkov JT. Penfold J. Thomas RK. Cox AR. Hedges N. Adsorption of hydrophobin –protein mixtures at the air-water interface: the impact of pH and electrolyte. *Langmuir*. 2015; 31: 10008-10016
- (89) Tucker IM. Petkov JT. Penfold J. Thomas RK. Cox AR. Hedges N. Adsorption of hydrophobin /  $\beta$ -casein mixtures at the solid-liquid interface. *J. Coll. Int. Sci*. 2016; 478: 81-87
- (90) Taylor DJF. Thomas RK. Penfold J. Adsorption of polymer-surfactant mixtures at the air-water interface. *Adv. Coll. Int. Sci*. 2007; 132: 69-110
- (91) Thomas RK. Penfold J. Thermodynamics at the air-water interface of mixtures of surfactants with polyelectrolytes, oligoelectrolytes, and multivalent metal electrolytes. *J. Phys. Chem. B*. 2018; 122: 12411-12427
- (92) Thomas RK. Penfold J. Li PX. Xu H. Multilayers formed by polyelectrolyte-surfactant and related mixtures at the air-water interface. *Adv. Coll. Int. Sci*. 2019; 269: 43-86
- (93) Wang L. Bouillon C. Cox A. Dickinson E. Durga K. Murray BS. Xu R. Interfacial study of class II hydrophobin and its mixtures with milk proteins. *J. Agric. Food Chem*. 2013; 61: 1554-1562
- (94) Tucker IM. Petkov JT. Penfold J. Thomas RK. Li PX. Cox AR. Hedges N. Webster JRP. Spontaneous surface self-assembly in protein-surfactant mixtures: interactions between hydrophobin and ethoxylated polysorbate surfactants. *J. Phys. Chem. B*. 2014; 118: 4867-4875
- (95) Penfold J. Thomas RK. Li PX. Petkov JT. Tucker IM. Cox AR. Hedges N. Webster JRP. Skoda MWA. Impact of the degree of ethoxylation of the ethoxylated polysorbate surfactant on the surface self-assembly in hydrophobin – ethoxylated polysorbate surfactant mixtures. *Langmuir*. 2014; 30: 9741-9751
- (96) Shen L. Guo A. Zhu X. Tween surfactants: adsorption, self-organisation and protein resistance. *Surf. Sci*. 2011; 605: 6085-6091

- (97) Ruiz-Henestrosa VP. Sanchez CC. Patino JMR. Adsorption and foaming characteristics of soy globulins and Tween 20 mixed systems. *Ind. Eng. Chem. Res.* 2008; 47: 2871-2885
- (98) Webb SD. Cleland JL. Carpenter JF. Randolph TWA. A new mechanism for decreasing aggregation in recombinant human interferon- $\gamma$  by a surfactant. *J. Pharm. Sci.* 2002; 91: 543-588
- (99) Zadymova NM. Yamplskaya GP. Filatova LY. Interaction of bovine serum albumin with nonionic surfactant Tween 80 in aqueous solution: complexation and association. *Colloid J.* 2006; 68: 162-172
- (100) Joshi O. McGuire J. Adsorption behaviour of lysozyme and Tween 20 at hydrophilic and hydrophobic silica-water interfaces. *Appl. Biochem. Biotechnol.* 2009; 152: 235-248
- (101) Penfold J. Thomas RK. Li PX. Petkov JT. Tucker I. Webster. JRP. Terry AE. Adsorption at the air-water and oil-water interfaces and self-assembly in aqueous solution of ethoxylated polysorbate nonionic surfactants. *Langmuir.* 2015; 31: 3003-3011
- (102) Graca M. Bongaerts JHH. Stokes JR. Granick S. Friction and adsorption of aqueous polyoxyethylene (Tween) surfactants on hydrophobic surfaces. *J. Coll. Int. Sci.* 2007; 315: 662-670
- (103) Prime KL. Whitesides GM. Adsorption of protein onto surfaces containing end-attached oligo(ethylene oxide): a model system using self-assembled monolayers. *J. Am. Chem. Soc.* 1993; 115: 10714-10721
- (104) Crilly JF. Russell AB. Cox AR. Cebula DJ. Designing multiscale structures for desired properties in ice cream. *Ind. Eng. Chem. Res.* 2008; 47: 6362-6367
- (105) Otzen D. Protein-surfactant interactions: a tale of many states. *Biochim. Biophys. Acta.* 2011; 1814: 562-592
- (106) Perriman AW. Mann S. Liquid proteins- a new frontier for biomolecular-based nanoscience. *ACS Nano.* 2011; 5: 6085-6091